JACS ARTICLES

Published on Web 04/16/2010

Loading Pentapod Deca(organo)[60]fullerenes with Electron Donors: From Photophysics to Photoelectrochemical Bilayers

Yutaka Matsuo,*[,†,‡] Takahiko Ichiki,[†] Shankara Gayathri Radhakrishnan,[§] Dirk M. Guldi,*[,§] and Eiichi Nakamura*[,†,‡]

Department of Chemistry, The University of Tokyo, Hongo, Bunkyo-ku, Tokyo 113-0033, Japan, Nakamura Functional Carbon Cluster Project, ERATO, Japan Science and Technology Agency, Hongo, Bunkyo-ku, Tokyo 113-0033, Japan, and Department of Chemistry and Pharmacy and Interdisciplinary Center for Molecular Materials, Friedrich-Alexander-Universität, Erlangen-Nürnberg, Germany

Received November 25, 2009; E-mail: matsuo@chem.s.u-tokyo.ac.jp; dirk.guldi@chemie.uni.erlangen.de; nakamura@chem.s.u-tokyo.ac.jp

Abstract: A pentapod deca(aryl)[60]fullerene, $C_{60}(C_6H_4CO_2H)_5(C_6H_4Fc)_5Me_2$ (**4**; Fc = ferrocenyl), bearing five carboxylic acid and five ferrocenyl groups was synthesized through top and bottom functionalization of [60]fullerene by means of copper-mediated penta-addition reactions. For electrochemical measurements (i.e., $E_{ox} = 0.08$ V, five-electron oxidation of the ferrocenyl groups; $E_{red} = -1.89$ and -2.28 V for the fullerene part vs Fc/Fc^+), we used an ester-protected compound, $C_{60}(C_6H_4CO_2Et)_5(C_6H_4Fc)_5Me_2$ (**2**), and **4** was probed by performing femtosecond flash photolysis experiments in a variety of organic solvents. Importantly, the formation of a radical ion pair state was corroborated with lifetimes of up to 333 ps in toluene. In complementary studies, penta(carboxylic acid)−penta(ferrocenyl) compound **4** was deposited on indium−tin oxide (ITO) electrodes with a surface coverage (i.e., 0.14 nmol/cm^2) that corresponded to a unique bilayer structure. Decisive for the bilayer motif is the presence of five ferrocenyl groups, which are assembled with a merry-go-round-shaped arrangement on the [60]fullerene. The novel **4**/ITO photoelectrode gave rise to a cathodic photocurrent with a 12% quantum yield in the presence of methyl viologen, whereas an anodic photocurrent was generated in the presence of ascorbic acid for a $C_{60}(C_6H_4CO_2H)_5(C_6H_5)_5Me_2$ (**5**)/ITO photoelectrode. Photophysical investigations revealed that the difference in photocurrent, that is, cathodic versus anodic photocurrents, is related to the nature of the excited state feature in **4** (i.e., charge separated state) and **5** (i.e., triplet excited state). The unique molecular architecture of **4**, in combination with its remarkable donor−acceptor properties, validates the use of the pentapod deca(aryl)[60]fullerene in photoelectrochemically active molecular devices.

Introduction

Harnessing the inexhaustible light of the sun—as observed in the natural photosynthetic machinery—offers myriad incentives to convert solar power into chemical energy.[1] Notably, in photosynthesis, cascades of short-range energy transfer and electron transfer events occur between well-arranged organic pigments and other cofactors. Thereby, the antenna portion captures light and transduces the resulting excitation energy, via singlet−singlet energy transfer, to the reaction center. In the latter, charges are then separated with remarkable efficiency to yield a spatially and electronically well-isolated radical pair.

In recent years, there has been considerable interest in electron donor−acceptor systems, in which C_{60} serves as electron and energy acceptors upon photoexcitation.[2] While a large variety of such systems have been synthesized and subjected to photophysical investigation,[2,3] the greatest attention has been paid to linked systems, in which C_{60} derivatives are molecular architectures ideally suited for devising integrated, multicomponent-model systems for transmitting and processing solar energy.[4] The implementation of C_{60} as a three-dimensional electron acceptor holds great hopes because of its small reorganization energy in electron transfer reactions, which has exerted a noteworthy impact on the development of C_{60}-based materials for applications involving light-induced charge separa-

[†] The University of Tokyo.
[‡] Nakamura Functional Carbon Cluster Project, ERATO, Japan Science and Technology Agency.
[§] Friedrich-Alexander-Universität.

(1) (a) Chen, L.-M.; Hong, Z.; Li, G.; Yang, Y. *Adv. Mater.* **2009**, *21*, 1434–1449. (b) Araki, Y.; Ito, O. *J. Photochem. Photobiol., C.* **2008**, *9*, 93–110. (c) Guenes, S.; Neugebauer, H.; Sariciftci, N. S. *Chem. Rev.* **2007**, *107*, 1324–1338. (d) Koeppe, R.; Sariciftci, N. S. *Photochem. Photobiol. Sci.* **2006**, *5*, 1122–1131.

(2) (a) Elim, H. I.; Jeon, S.-H.; Verma, S.; Ji, W.; Tan, L.-S.; Urbas, A.; Chiang, L. Y. *J. Phys. Chem. B* **2008**, *112*, 9561–9564. (b) Imahori, H.; Sakata, Y. *Adv. Mater.* **1997**, *7*, 537–546. (c) Brabec, C., Scherf, U., Dyakonov, V., Eds. *Organic Photovoltaics*; Wiley-VCH: Weinheim, 2008, pp 155−178.

(3) (a) Fukuzumi, S.; Kojima, T. *J. Mater. Chem.* **2008**, *18*, 1427–1439. (b) Imahori, H. *Org. Biomol. Chem.* **2004**, *2*, 1425–1433. (c) Guldi, D. M. *Chem. Soc. Rev.* **2002**, *21*, 22–36.

(4) (a) Imahori, H.; Hagiwara, K.; Akiyama, T.; Aoki, M.; Taniguchi, S.; Okada, T.; Shirakawa, M.; Sakata, Y. *Chem. Phys. Lett.* **1996**, *263*, 545–550. (b) Fukuzumi, S.; Ohkubo, K.; Imahori, H.; Guldi, D. M. *Chem.—Eur. J.* **2003**, *9*, 1585–1593. (c) Guldi, D. M. *Spectrum* **2003**, *16*, 8–11.

 10.1021/ja909970h

tion. In fact, in multicomponent electron donor−acceptor conjugates, the successful mimicry of the primary events in photosynthesis has been realized. Once embedded in a highly viscose environment, C_{60}-H_2P-$(ZnP)_3$ reveals the following key processes: (i) light harvesting by the antennas, (ii) unidirectional energy transfer to the reaction center, (iii) efficient charge separation to yield a transient radical ion pair, (iv) charge migration to generate spatially distant radical ion pairs, and finally, (v) charge recombination in a time regime that enables the utilization of its chemical potential for catalytic reactions. These examples indicate that the donor and acceptor choices and their tailored arrangement are essential for controlling the photoelectrochemical functions.[3,5]

The construction of multifunctional hybrid cells, which are integrated using electron donor−acceptor conjugates/hybrids and can be employed in photoelectrochemical solar energy conversion, constitutes one of the most ambitious research objectives of our time.[6] However, to produce electrical energy as a consequence of light-triggered charge separation, a judicial arrangement of the molecules against the electrodes is important. In this context, the preparation of a self-assembled monolayer (SAM)[7] is particularly promising. In fact, we recently reported on a novel photocurrent conversion system based on SAMs of pentapod penta(organo)[60]fullerene derivatives[8] on an indium−tin oxide electrode.[9] Interestingly, the photocurrent direction was found to depend distinctly on the positional relationship between the electron-accepting C_{60} and the metal atoms as electron donors.

Because of the placement of the 10 aryl groups, which create large, rigid, hand-drum-shaped dendritic structures, deca(organo)[60]fullerene derivatives[10] offer a unique platform to gain full control over the positional relation of the donor and acceptor components.[11] In addition, the core is an attractive alternative for the hoop-shaped 40π-electron cyclophenacene system, which exhibits outstanding photophysical properties.[12] Herein, we report on a novel pentapod deca(organo)[60]fullerene electron donor−acceptor conjugate that has been immobilized on semiconducting ITO electrodes; the conjugate consists of a

Scheme 1

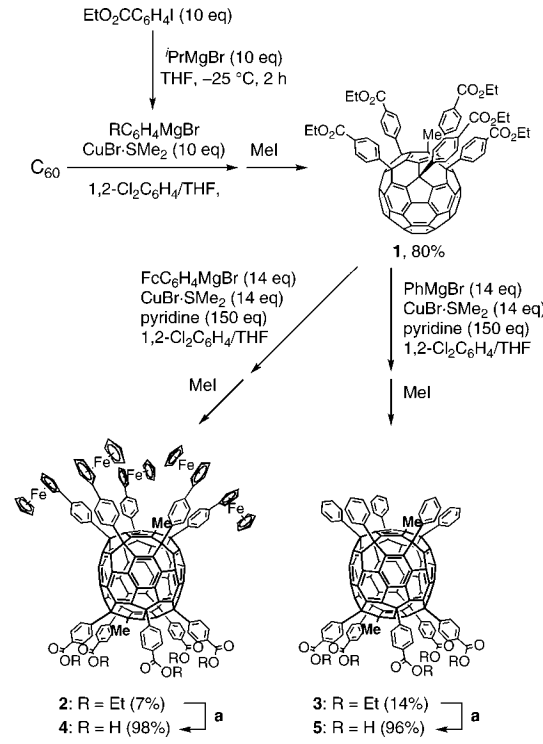

core[10] cyclophenacene structure, used as a hoop-shaped benzenoid acceptor and five ferrocenyl groups as donors. A key asset for the new pentapod deca(organo)[60]fullerene is the dendritic arrangement of the five ferrocene moieties on the top part of the C_{60}. In particular, this assists in retarding energy wastage and undesired charge recombination and in achieving a unique bilayer structure on the ITO. Both features are crucial for efficient photocurrent generation.

Results and Discussion

Synthesis and Electrochemical Properties. We first describe the synthesis of deca(aryl)[60]fullerenes bearing five ferrocenyl and five ester groups. The regioselective reaction of an ethoxycarbonylphenyl copper reagent (10 equiv) with [60]fullerene at 35 °C under the previously described conditions,[13] followed by methylation, produced the penta adduct **1** in 80% yield (Scheme 1). Compound **1** was subjected to the second-stage penta-addition of a ferrocenylphenyl copper reagent in the presence of pyridine and the subsequent methylation process to obtain the decaaryl adduct $C_{60}(C_6H_4CO_2Et)_5(C_6H_4Fc)_5Me_2$ (**2**; Fc = ferrocenyl), its regioisomer, and octaaryl adducts.[10c] The product **2** was purified by the use of preparative HPLC. The isolated yield of **2** was low (7%) because of the predominant formation of the regioisomer in the addition.[10c] A reference decaaryl compound $C_{60}(C_6H_4CO_2Et)_5Ph_5Me_2$ (**3**) that we used as a reference compound for the photophysical study was synthesized in the same manner.

A cyclic voltammetric (CV) analysis of **2** was performed to investigate the donor−acceptor properties of the molecule (Figure 1a). Compound **2** showed a single reversible five-electron oxidation wave because of the five ferrocenyl groups at 80 mV vs Fc/Fc^+, which is slightly shifted to the positive side against the ferrocene/ferrocenium couple reference. The

(5) (a) D'Souza, F.; Ito, O. *Coord. Chem. Rev.* **2005**, *249*, 1412–1422. (b) Guldi, D. M.; Imahori, H. *J. Porphyrins Phthalocyanines* **2004**, *8*, 976–983.
(6) (a) Bonifazi, D.; Enger, O.; Diederich, F. *Chem. Soc. Rev.* **2007**, *36*, 390. (b) Umeyama, T.; Imahori, H. *Photosynth. Res.* **2006**, *87*, 63–71. (c) Sakata, Y.; Imahori, H.; Sugiura, K.-I. *J. Incl. Phenom. Macrocycl. Chem.* **2001**, *41*, 31–36. (d) Huang, C.-H.; McClenaghan, N. D.; Kuhn, A.; Bravic, G.; Bassani, D. M. *Tetrahedron* **2006**, *62*, 2050–2059.
(7) Ulman, A. *Chem. Rev.* **1996**, *96*, 1533–1554.
(8) (a) Sawamura, M.; Iikura, H.; Nakamura, E. *J. Am. Chem. Soc.* **1996**, *118*, 12850–12851. (b) Matsuo, Y.; Muramatsu, A.; Tahara, K.; Koide, M.; Nakamura, E. *Org. Synth.* **2006**, *83*, 80–87. (c) Matsuo, Y.; Nakamura, E. *Chem. Rev.* **2008**, *108*, 3016–3028.
(9) Matsuo, Y.; Kanaizuka, K.; Matsuo, K.; Zhong, W.-Y.; Nakae, T.; Nakamura, E. *J. Am. Chem. Soc.* **2008**, *130*, 5016–5017.
(10) (a) Nakamura, E.; Tahara, K.; Matsuo, Y.; Sawamura, M. *J. Am. Chem. Soc.* **2003**, *125*, 2834. (b) Matsuo, Y.; Tahara, K.; Nakamura, E. *Org. Lett.* **2003**, *5*, 3181. (c) Matsuo, Y.; Tahara, K.; Sawamura, M.; Nakamura, E. *J. Am. Chem. Soc.* **2004**, *126*, 8725. (d) Matsuo, Y.; Nakamura, E. Cyclophenacene Cut Out of Fullerene. In *Functional Organic Materials: Syntheses, Strategies and Applications*; Müller, T. J. J., Bunz, U. H. F., Eds., Wiley-VCH, Weinheim, 2007, pp 59−80. (e) Matsuo, Y.; Tahara, K.; Morita, K.; Matsuo, K.; Nakamura, E. *Angew. Chem., Int. Ed.* **2007**, *46*, 2844. (f) Matsuo, Y.; Fujita, T.; Nakamura, E. *Chem. Asian J.* **2007**, *2*, 948. (g) Matsuo, Y. *Bull. Chem. Soc. Jpn.* **2008**, *81*, 320–330.
(11) Zhang, X.; Matsuo, Y.; Nakamura, E. *Org. Lett.* **2008**, *10*, 4145–4147.
(12) Matsuo, Y.; Sato, Y.; Hashiguchi, M.; Matsuo, K.; Nakamura, E. *Adv. Funct. Mater.* **2009**, *19*, 2224–2229.
(13) Zhong, Y.-W.; Matsuo, Y.; Nakamura, E. *Org. Lett.* **2006**, *8*, 1463–1466.

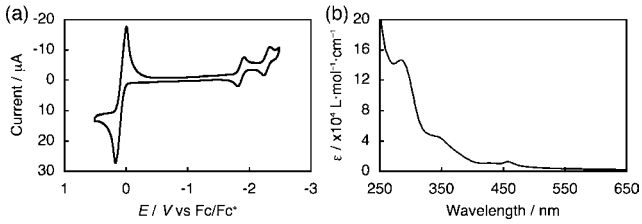

Figure 1. Electrochemical and photophysical properties of **2**. (a) CV of **2** at 25 °C in THF solution containing $^{n}Bu_4NClO_4$ as supporting electrolyte. $E_{ox} = 0.08$ V, $E_{red1} = -1.89$ V, $E_{red2} = -2.28$ V vs Fc/Fc^{+}. (b) UV−vis absorption spectrum of **2**.

results indicate that the five ferrocene groups exert an electron-withdrawing effect on the fullerene moiety.

The compound also showed two reversible one-electron reduction waves because of the fullerene part at −1.89 and −2.28 V. The first and second reduction potentials for the fullerene core shifted to the positive side compared with those of the reference compound **3** (−2.03 and −2.48 V) because of the electron-withdrawing nature of the ferrocenyl unit in the ground state.

Photophysics and Intramolecular Charge Separation Properties. Initially, non-ferrocenyl and ferrocenyl compounds **3** and **2** were examined in depth by both steady-state and time-resolved fluorescence spectroscopy in a variety of solvents at room temperature. Compound **3**, which gives rise to a characteristic fluorescence maximum at 568 nm (Figure S1, Supporting Information), fluorescence quantum yield of 6×10^{-2}, and fluorescence lifetime of 75 ns in toluene, was used as an internal reference system. Notably, there is a marked increase in the fluorescence quantum yield and lifetime relative to those of pristine C_{60} (2×10^{-4} and 1.4 ns);[14] this increase is attributed to its extensive functionalization, which alters its electronic structure.[10] Compound **2** showed a significant quenching of the fullerene-centered fluorescence (quantum yield $\sim 10^{-5}$). It is important to note that despite the overall quenching, the fluorescence patterns of **2** and **3** are superimposable (data not shown). However, a closer look reveals subtle changes in the fluorescence of **2** as the solvent polarity is increased from toluene to THF. In fact, the lower fluorescence quantum yields in THF compared with toluene are indicative of an increasingly accelerated singlet excited state decay. Implicit is an intramolecular charge transfer deactivation induced by the electron-donating ferrocenes. This hypothesis was further supported by the lack of detectable fluorescence beyond 0.1 ns, which is the temporal resolution of our instrumental setup. A notable exception is the outcome in methylcyclohexane with a quantum yield of 3×10^{-3} and a lifetime of 11 ns.

Next, transient absorption measurements[15] were performed in cyclohexane, toluene, anisole, THF, and benzonitrile to provide mechanistic insights into the singlet excited state deactivation in the absence and presence of the ferrocene groups. Following the time evolution of the characteristic singlet excited state features of C_{60} is a sensitive means to identify spectral features of the resulting photoproducts and to determine absolute rate constants for the intramolecular decay.

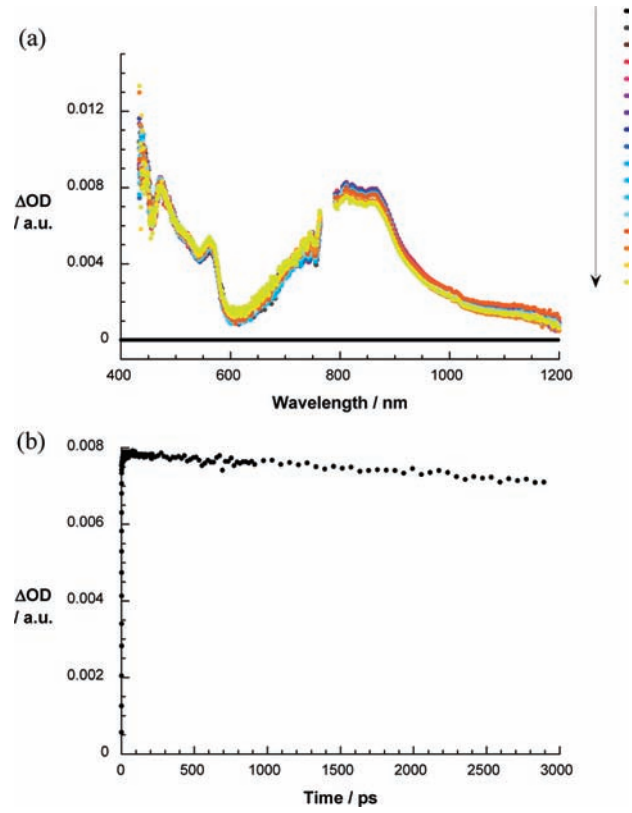

Figure 2. Time-resolved photophysical data for the reference compound **3**. (a) Differential absorption spectra (visible and near-infrared) obtained upon femtosecond flash photolysis (387 nm) of **3** (10^{-6} M) in toluene with several time delays between 0 and 3000 ps (time course: from gray, red, blue, yellow to black lines; see figure legend for time evolution) at room temperature. (b) Time-absorption profiles of spectra at 850 nm.

We first looked at the transient absorption spectra following the 387 nm excitation of **3**. Figure 2a illustrates, for example, the differential absorption changes that were recorded in the visible and near-infrared region spectra in toluene. Commencing with the conclusion of the photoexcitation, the excited-state features are seen, especially in the near-infrared region, where distinct maxima evolve at 820 and 870 nm. The visible region, on the other hand, is dominated by maxima at 475 and 565 nm. These spectral attributes are indicative of the singlet excited state of **3**, which is formed nearly instantaneously (i.e. >1 ps) (Figure 2b); this state presumably involves an internal deactivation commencing with higher-lying electronic or vibrational excited states. However, a multiwavelength analysis of the singlet decay in the visible and near-infrared region indicates that the singlet excited state is long-lived. The absence of any appreciable decays infer that its lifetime is well beyond the experimental time window of 3.0 ns. In line with the fluorescence measurements, a rather inefficient intersystem crossing is likely to be operative. In fact, a complementary nanosecond experiment confirmed the slow nature of the spin-forbidden singlet-to-triplet transformation. From the spectral changes, as they were recorded with a time delay of, for example, 10 ns (see Figure S2, Supporting Information), we derive an extraordinarily long-lived singlet excited state (i.e., 100 ± 5 ns). On the other hand, the energetically lower-lying triplet excited state

(14) (a) Anderson, J. L.; An, Y.-Z.; Rubin, Y.; Foote, C. S. *J. Am. Chem. Soc.* **1994**, *116*, 9763–9764. (b) Arbogast, J. W.; Darmanyan, A. P.; Foote, C. S.; Rubin, Y.; Diederich, F. N.; Alvarez, M. M.; Anz, S. J.; Whetten, R. L. *J. Phys. Chem.* **1991**, *95*, 11–12.

(15) (a) Guldi, D. M.; Rahman, G. M. A.; Marczak, R.; Matsuo, Y.; Yamanaka, M.; Nakamura, E. *J. Am. Chem. Soc.* **2006**, *128*, 9420–9427. (b) Marczak, R.; Wielopolski, M.; Gayathri, S. S.; Guldi, D. M.; Matsuo, Y.; Matsuo, K.; Tahara, K.; Nakamura, E. *J. Am. Chem. Soc.* **2008**, *130*, 16207–16215. (c) Matsuo, Y.; Maruyama, M.; Gayathri, S. S.; Uchida, T.; Guldi, D. M.; Kishida, H.; Nakamura, A.; Nakamura, E. *J. Am. Chem. Soc.* **2009**, *131*, 12643–12649.

reveals a transient maximum at 610 nm (Figure S2, Supporting Information). Under anaerobic conditions, the triplet lifetimes are ~20 μs.

When probing **2** in transient absorption measurements, it is of particular importance that the C_{60} singlet excited state with maxima at 475, 565, 820, and 870 nm is discernible. This finding attests the successful photoexcitation of C_{60} despite the presence of several ferrocenes. In stark contrast to **3**, the singlet excited state features in **2** are metastable, even on the 3 ns time scale. In particular, we observed the occurrence of a solvent-dependent decay, which ranges from 5 ps in benzonitrile to approximately 11000 ps in methylcyclohexane.

The picosecond experiments in toluene and benzonitrile (Figure 3a,b) exhibited a series of absorption bands that include a strong maximum at 620 nm followed by a weaker maximum at 855 nm. The former almost corresponds to the absorption because of reduced species[16] for the central π-conjugated system ([10]cyclophenacene). The latter evolve with practically identical kinetics to that of the singlet excited state decay. It is important to note that complementary pulse radiolytic reduction experiments with **3** resulted in a transient maximum at 615 nm formed under pseudo first-order conditions. In accordance with these results, we propose that, indeed, a charge transfer evolves from the C_{60} singlet excited state and, in turn, creates the radical ion pair state, which is responsible for the fast intramolecular deactivation of photoexcited **2**.

Figure 3c shows that in methylcyclohexane, the radical ion pair state does not form. Instead, we confirmed the excited state features of the long-lived (5 μs) triplet (605 nm) in complementary nanosecond experiments (data not shown).

It is safe to assume that the driving force for charge transfer in methylcyclohexane is insufficient to compete with the intersystem crossings. In fact, consideration of the energies of the radical ion pair state and the singlet excited state, with values of 1.97 and 2.18 eV, respectively, supports the notion of an endothermic charge transfer but exothermic intersystem crossing. This is apparently different in toluene, anisole, THF, and benzonitrile—with energies of the radical ion pair state as low as 1.64 eV—where the charge separation occurs with kinetics that are nearly 2 orders of magnitude faster than the intersystem crossing.

The radical ion pair states in the different solvents decay back to the ground state on a time scale of several hundred picoseconds (Figure 3d). In toluene, anisole, THF, and benzonitrile, we determined radical ion pair lifetimes of 333, 233, 135, and 162 ps, respectively.

Deposition of 4 on ITO and Photocurrent Generation. As described above, the hand-drum-shaped compound **2** has a longer lifetime for the charge separated state (up to 333 ps) than the previous pentapod penta(organo)[60]fullerene systems (30−40 ps).[15] This feature raises the important question of whether the merry-go-round-like structure constructed on the top part of the fullerene favorably influences the assembled structures on the substrate, thereby increasing the efficiency of the photocurrent generation. To address this question, we hydrolyzed the five ester moieties of **2** and **3** with NaOH to obtain pentacarboxylic acid molecules, $C_{60}(C_6H_4CO_2H)_5(C_6H_4Fc)_5Me_2$ (**4**) and $C_{60}(C_6H_4CO_2H)_5(C_6H_5)_5Me_2$ (**5**), so that we could deposit these molecules on the ITO surface, forming COO−metal bonds. The deposition was done by the immersion of an ITO substrate (treated by ozone just before use) in a THF solution (0.1 mM) of **4** and **5** as described previously for our related studies.[9,18]

CV analysis of **4**/ITO gave us information on the time course of the deposition of **4** and the number of the molecules per cm^2. A reversible oxidation process occurred at 0.17 V (vs Ag/Ag$^+$), almost equal to the value determined for the solution of **2**, and was assigned to the oxidation of the five ferrocenyl groups. The surface coverage of **4** on the ITO was determined by the integration of anodic charge in the voltammogram at a sweep rate of 0.1 V/s (Figure 4a, black dots). The speed of deposition was qualitatively the same as that observed previously for pentapod carboxylic acid molecules,[9] except that the surface coverage continued to increase after the first two layers were deposited and stopped after the formation of approximately four layers. Thus, the density of the molecules increased first to ~0.15 nmol/cm^2 then to ~0.29 nmol/cm^2 (Figure 4a, black dots). The former value is almost twice as large, and the latter about 4 times as large, as that reported for a monolayer of the pentapod derivatives (0.07−0.1 nmol/cm^2).[9] Subsequent measurements on the properties of the thick layer tended to give erratic data, suggesting that it is physically or chemically unstable. Hence, the samples were sonicated to check if more stably deposited samples could be obtained.

When the **4**/ITO sample was sonicated for 10 min in between each measurement during deposition (Figure 4a, red dots), it was found that the deposition stopped after formation of two layers. Thus, the coverage density increased only for the first five days (Figure 4a). Sonication of the sample for 30 min gave the same density time profile, indicating that the first two layers of **4** are in fact very stable. The standard peak-scan rate relationship experiment[17] carried out for the sonicated (10 min) sample clearly showed nonlinearity, indicating that more than one layer of **4** was deposited on ITO (Figure S3, Supporting Information).

We noted that the hand-drum molecule **4** shows a strong tendency to aggregate in THF solution (*Z*-average =127.4 nm) determined by a dynamic light scattering experiment of the 0.1 mM solution). On the basis of this aggregation behavior, the strong propensity of structurally related polar fullerenes to form a head-to-head bilayer,[19] the density of coverage, the time profile of the deposition, and the sonication effects, we consider that the molecules deposit as a pair of bilayer, presumably as illustrated in parts b and c of Figure 4. The second bilayer deposits on the first through hydrogen bonding (Figure 4d), which is probably much weaker than the COO-metal bonding that connects the bottom layer to the ITO surface.

Photocurrent generation experiments on the sonicated **4**/ITO device were carried out in a degassed 0.1 M Na_2SO_4 aqueous solution containing 50 mM ascorbic acid (AsA) as an electron donor or methyl viologen (MV^{2+}) as an electron acceptor (Figure 5). The **4**/ITO device serves as the working electrode in a cell that has a platinum counter electrode and a Ag/AgCl (satd. KCl) reference electrode. In an experiment in the presence of MV^{2+}, a stable cathodic photocurrent was generated upon light irradia-

(16) Matsuo, Y.; Tahara, K.; Nakamura, E. *J. Am. Chem. Soc.* **2006**, *128*, 7154–7155.

(17) Kuramitz, H.; Sugawara, K.; Kawasaki, M.; Hasebe, K.; Nakamura, H.; Tanaka, S. *Anal. Sci.* **1999**, *15*, 589–592.

(18) (a) Sakamoto, A.; Matsuo, Y.; Matsuo, K.; Nakamura, E. *Chem. Asian J.* **2009**, *4*, 1208–1212. (b) Chen, T.; Pan, G.-B.; Yan, H.-J.; Wan, L.-J.; Matsuo, Y.; Nakamura, E. *J. Phys. Chem. C* **2010**, *114*, 3170–3174.

(19) (a) Zhou, S.; Burger, C.; Chu, B.; Sawamura, M.; Nagahama, N.; Toganoh, M.; Hackler, U. E.; Isobe, H.; Nakamura, E. *Science* **2001**, *291*, 1944–1947. (b) Isobe, H.; Homma, T.; Nakamura, E. *Proc. Natl. Acad. Sci. U.S.A.* **2007**, *104*, 14895–14898.

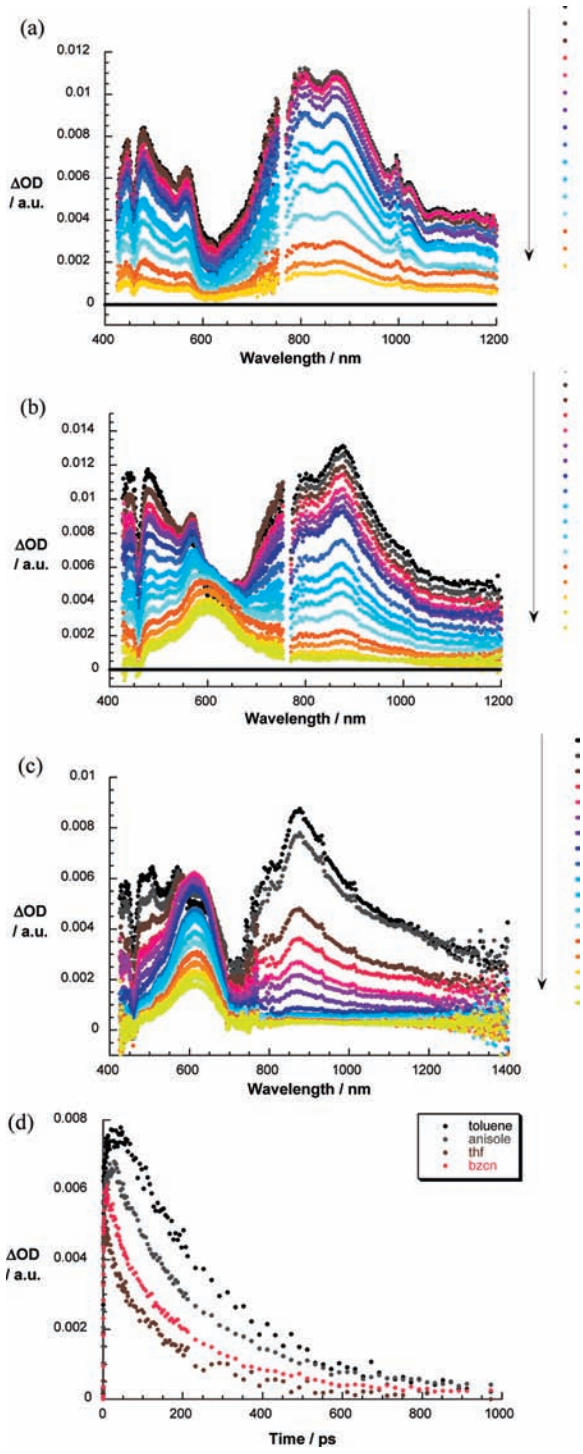

Figure 3. Time-resolved photophysical data for compound **2**. (a) Differential absorption spectra (visible and near-infrared) obtained upon femtosecond flash photolysis (387 nm) of **2** (10^{-6} M) in methylcyclohexane with several time delays between 0 and 3000 ps (time course: from gray, red, blue, yellow to black lines - see figure legend for time evolution) at room temperature. (b) Differential absorption spectra (visible and near-infrared) obtained upon femtosecond flash photolysis (387 nm) of **2** (10^{-6} M) in toluene with several time delays between 0 and 3000 ps (time course: from gray, red, blue, yellow to black lines - see figure legend for time evolution) at room temperature. (c) Differential absorption spectra (visible and near-infrared) obtained upon femtosecond flash photolysis (387 nm) of **2** (10^{-6} M) in benzonitrile ith several time delays between 0 and 3000 ps (time course: from gray, red, blue, yellow to black lines - see figure legend for time evolution) at room temperature. (d) Time-absorption profiles monitoring the charge separation and charge recombination dynamics in the several solvents at 600 nm.

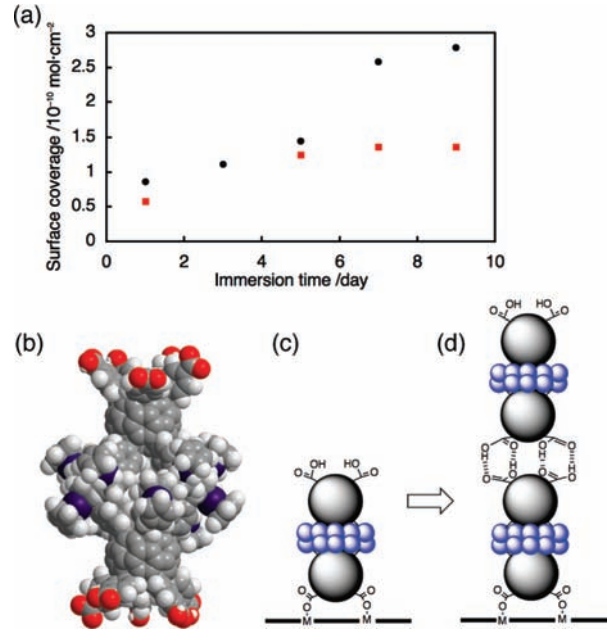

Figure 4. Deposition of the pentacarboxylic acid **4** on ITO. (a) Surface coverage−immersion time relationship for the bilayer of **4**. Black and red dots denote layer formation without and with sonication, respectively. (b) A plausible molecular model of bimolecular van der Waals stacking of **4**. (c) Bilayer on ITO bonded by metal−carboxylate formation (M = Sn or In) and ferrocene−ferrocene van der Waals interaction. (d) Hydrogen bonding between two bilayers.

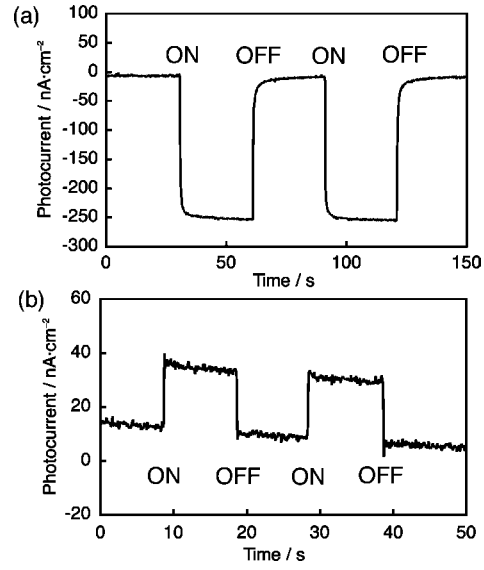

Figure 5. Photoelectrochemical properties of pentapod molecules on ITO electrode surfaces. (a) Cathodic photocurrent generation of **4**/ITO (sonicated) in the presence of MV^{2+} in aqueous solution containing Na_2SO_4 at −100 mV applied bias voltage vs Ag/AgCl reference electrode. (b) Anodic photocurrent generation of reference system **5**/ITO in the presence of AsA.

tion ($\lambda_{ex} = 400 \pm 10$ nm, with a power of 307 μW) at an applied potential of −100 mV versus Ag/AgCl (Figure 5a). The observed photocurrent density of −250 nA/cm^2 is about 4 times as large as that reported for a monolayer of pentacarboxylic acid molecules lacking the pentaferrocenyl groups (e.g., −65 nA/cm^2), and the quantum yield per molecule was 12%, which is nearly twice as large (up to 6.3%).[9,18a] Photocurrent action spectra at a −100 mV bias versus Ag/AgCl were measured (Figure S4, Supporting Information), which matched well with

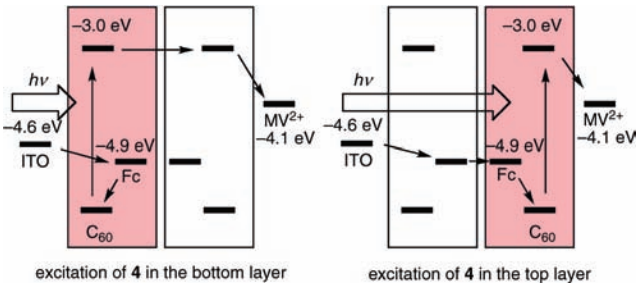

Figure 6. A plausible energy diagram for photoexcitation of each layer of the bilayer of **4**/ITO that contributes to the increase in photocurrent generation. The LUMO of **4** is based on the CV data. The work function of ITO was obtained by using photoelectron yield spectrometry.[20]

the corresponding absorption spectrum of **2** in solution (Figure 1b), indicating that the fullerene compound **4** is responsible for the photocurrent conversion.

No anodic photocurrent was observed for **4** in an experiment in the presence of AsA, while the reference compound **5** generated an anodic photocurrent (Figure 5b). Thus, the presence of ferrocene groups is responsible for the generation of the cathodic photocurrent.

We ascribe the generation of high current density in part to the molecular properties of **4** itself and in part to the bilayer structure. We suggest that the higher performance per molecule is due to the long lifetime of the charge-separated excited state, from which electron and hole dissociate intermolecularly to generate the photocurrent. In addition, the high current density suggests that there is additivity of the photocurrent generation by each layer in the bilayer (Figure 6); that is intermolecular excited state quenching within the bilayer does not intervene in the photocurrent generation process due to the very fast intramolecular conversion of the singlet excited state to the long-lived charge-separated state (see above).

Conclusion

In this study, we synthesized the pentapods: deca(organo)[60]fullerene bearing five ferrocenyl groups (**2** and **4**) and studied their photophysical and photochemical properties in solution and on an electrode surface. The multiple-donor−acceptor molecule **2** exhibited a charge separation lifetime that was approximately 10 times longer (up to 333 ps) than the previous pentapod penta(organo)[60]fullerene systems. The pentacarboxylic acid molecule **4** was fixed on the ITO electrode surface to form a bilayer device. This device generated a cathodic photocurrent that shows a 4 times larger current density and a twice larger density/molecule (quantum yield of 12%) than those reported for the devices using similar pentapod fullerenes lacking the pentaferrocenyl groups. Given the above results and the unique photoelectrochemical properties of the cyclophenacene framework, we expect that this hand-drum motif will be useful for the construction of a variety of photoelectrochemically active molecular devices[21] and photocurrent generating devices.[22]

Experimental Section

General. Syntheses were carried out under a nitrogen or argon atmosphere with standard Schlenk techniques. The water contents of the solvents were determined, using a Karl Fischer moisture titration (MK-210, Kyoto Electronics Co.), to be less than 30 ppm. All of the reactions were monitored by HPLC (column, RP-FULLERENE, 4.6 mm × 250 mm, Nacalai Tesque; flow rate, 2.0 mL/min; eluent, toluene/acetonitrile; detector, Shimadzu SPD-M10Avp). Preparative HPLC was performed on a RP-FULLERENE, column (20 mm × 250 mm) using toluene/acetonitrile as the eluent (detected at 350 nm with a UV spectrophotometric detector, Shimadzu SPD-6A). The isolated yields were calculated on the basis of the starting fullerene compounds. The NMR spectra were measured with JEOL ECA-500 (500 MHz) instruments. Spectra are reported in parts per million from the internal tetramethylsilane (δ 0.00 ppm) or residual protons of the deuterated solvent for ^{1}H NMR, and from solvent carbon (e.g., δ 77.00 ppm for chloroform) for ^{13}C NMR. Mass spectra were measured on a JEOL JMS-T100LC APCI/ESI-TOF mass spectrometer.

Materials. Methyl viologen (MV^{2+}) was purchased from Sigma-Aldrich Co. and used as received. ^{n}Bu$_4$NClO$_4$, for electrochemical measurements, was purchased from Kanto Chemicals and used after recrystallization from ethanol. Na_2SO_4 and ascorbic acid were purchased from Kanto Chemicals and used as received. A THF solution of KO^{t}Bu was purchased from Sigma-Aldrich Co. Transparent indium−tin oxide (ITO) electrodes (10 W/cm^2, ITO on glass plate) were obtained from GEOMATEC Inc. (Japan).

Preparation of Molecular Layers on ITO. The preparation of self-assembled molecular layers of fullerene compounds was carried out using a simple dipping method: an ITO electrode (25 mm ×20 mm; UV−O_3 treated before use) was immersed in a 0.1 mM THF solution of the fullerene derivatives at room temperature. Then the ITO electrode was washed with THF and dried in an argon gas stream.

Electrochemical Measurements. Electrochemical measurements were carried out with a Hokuto HZ-5000 voltammetric analyzer. A glassy-carbon, a platinum coil, and a Ag/Ag^+ electrode were used as the working, counter, and reference electrodes, respectively, in THF with 0.1 M ^{n}Bu$_4$NClO$_4$ as the supporting electrolyte. CV was performed at a scan rate of 100 mV/s. The potential was corrected against a standard reference, the ferrocene/ferrocenium couple (Fc/Fc^+).

Procedure for the Synthesis of $C_{60}(C_6H_4Fc)_5Me(C_6H_4COOEt)_5Me$ (2). A solution of $C_{60}(C_6H_4COOEt)_5Me$ (147 mg, 0.100 mmol) in *o*-dichlorobenzene (3 mL) was added to a mixture of an organocopper reagent prepared from FcC_6H_4MgBr (3.5 mL of a 0.40 M solution in THF, 1.40 mmol) and copper bromide dimethyl sulfide (293 mg, 1.43 mmol) in THF (1.0 mL) and pyridine (1.2 mL) at room temperature. The resulting mixture was stirred until the starting material disappeared, as monitored by HPLC. MeI (0.5 mL) was then added, and the mixture was stirred for 2 h at 40 °C. After the removal of volatile materials under reduced pressure, the mixture was diluted with toluene (20 mL), filtered through a pad of silica gel, and concentrated. Purification by preparative HPLC afforded a yellow solid (**2**; 18.4 mg, 7% yield). APCI-HRMS (+): calcd for $C_{187}H_{117}O_{10}Fe_5$ [M^+ + H] 2801.5388, found 2801.5400.

Procedure for the Synthesis of $C_{60}Ph_5Me(C_6H_4COOEt)_5Me$ (3). A solution of $C_{60}(C_6H_4COOEt)_5Me$ (150 mg, 0.100 mmol) in *o*-dichlorobenzene (25 mL) was added to a mixture of an organocopper reagent prepared from PhMgBr (1.15 mL of a 0.96 M solution in THF, 1.1 mmol) and copper bromide dimethyl sulfide (246 mg, 1.20 mmol) in THF (25 mL) and pyridine (1.2 mL) at room temperature. The resulting mixture was stirred until the

(20) Niinomi, T.; Matsuo, Y.; Hashiguchi, M.; Sato, Y.; Nakamura, E. *J. Mater. Chem.* **2009**, *19*, 5804–5811.

(21) (a) Hasobe, T.; Imahori, H.; Kamat, P. V.; Fukuzumi, S. *J. Am. Chem. Soc.* **2003**, *125*, 14962–14963. (b) Cho, Y.-J.; Ahn, T. K.; Song, H.; Kim, K. S.; Lee, C. Y.; Seo, W. S.; Lee, K.; Kim, S. K.; Kim, D.; Park, J. T. *J. Am. Chem. Soc.* **2005**, *127*, 2380–2381. (c) Kira, A.; Umeyama, T.; Matano, Y.; Yoshida, K.; Isoda, S.; Park, J. K.; Kim, D.; Imahori, H. *J. Am. Chem. Soc.* **2009**, *131*, 3198–3200. (d) Subbaiyan, N. K.; Wijesinghe, C. A.; D'Souza, F. *J. Am. Chem. Soc.* **2009**, *131*, 14646–14647.

(22) Matsuo, Y.; Sato, Y.; Niinomi, T.; Soga, I.; Tanaka, H.; Nakamura, E. *J. Am. Chem. Soc.* **2009**, *131*, 16048–16050.

starting material disappeared, as monitored by HPLC. MeI (0.5 mL) was then added, and the mixture was stirred for 2 h at 40 °C. After the removal of volatile materials under reduced pressure, the mixture was diluted with toluene (100 mL), filtered through a pad of silica gel, and concentrated. Purification by preparative HPLC afforded yellow solids (**3**; 25 mg, 14% yield). APCI-HRMS (+): calcd for $C_{137}H_{77}O_{10}$ [M^+ + H] 1881.5511, found 1881.5524.

Procedure for the Synthesis of $C_{60}(C_6H_4Fc)_5Me(C_6H_4COOH)_5Me$ (4). A solution of NaOH in MeOH (0.5 M, 0.1 mmol, 0.2 mL) was added to a solution of **2** (18.0 mg, 0.006 mmol) in 5 mL of toluene. The mixture was heated to 60 °C and stirred for 1 h. After cooling to room temperature, the precipitate was collected by filtration and washed with hexane. The solid obtained was then treated with 2 mL of a 1 N HCl aqueous solution. After filtration and washing with water, the obtained solid was dried under vacuum (**4**; 16.8 mg, 98% yield). APCI-HRMS (+): calcd for $C_{177}H_{97}O_{10}Fe_5$ [M^+ + H] 2661.3823, found 2661.3863.

Procedure for the Synthesis of $C_{60}(C_6H_5)_5Me(C_6H_4COOH)_5Me$ (5). A solution of NaOH in MeOH (0.5 M, 0.1 mmol, 0.2 mL) was added to a solution of **3** (25.0 mg, 0.006 mmol) in 5 mL of toluene. The mixture was heated to 60 °C and stirred for 1 h. After cooling to room temperature, the precipitate was collected by filtration and washed with hexane. The solid obtained was then treated with 2 mL of a 1 N HCl aqueous solution. After filtration and washing with water, the obtained solid was dried under vacuum (**5**; 23.0 mg, 96% yield). APCI-HRMS (+): calcd for $C_{127}H_{57}O_{10}$ [M^+ + H] 1741.3946, found 1741.3955.

Photophysical Studies. Femtosecond transient absorption studies were performed using 387 nm laser pulses with a 150 fs pulse width, generated by a β-barium borate crystal upon higher-order nonlinear processes from an amplified Ti:sapphire laser system (CPA 2001 Laser, Clark-MXR Inc.) The white light was generated by a 2-mm sapphire crystal, and with the help of a delay line, a time delay between the pump and probe beam was created with high precision. Finally, the change in optical density (ΔOD) was measured against the wavelength in both the visible and near-infrared regions. Nanosecond laser flash photolysis experiments were performed with 337-nm laser pulses from a nitrogen laser (8-ns pulse width) using a front-face excitation geometry.

Characterization of the Molecular Layers. CV of the ITO modified with fullerene derivatives was carried out using an ITO working electrode, a Pt wire counter electrode, and a Ag/Ag^+ reference electrode in a 0.1 M CH_3CN solution containing $^nBu_4NClO_4$ as the supporting electrolyte in a standard one-compartment cell under argon. Figure 4a indicates the dependence of the surface coverage on the period of immersion for the assembly of **4** on the ITO electrode.

Photocurrent Measurement. Photoelectrochemical measurements of the fullerene molecules on the ITO electrodes were carried out in aqueous media containing the Na_2SO_4 electrolyte in a one-compartment cell, irradiated with monochromatic excitation light (the light intensity at 400 nm was 307 $\pm$ 5 mW for systems of ITO electrodes). The photocurrent was detected with an HZ-5000 voltammetric analyzer. Bias voltages were applied against a Ag/AgCl reference electrode.

Acknowledgment. This study was partially supported by KAKENHI (No. 18105004 and No. 18684014) and the Global COE Program for Chemistry Innovation of the MEXT, Japan. The Deutsche Forschungsgemeinschaft (Grant SFB 583), Cluster of Excellence "Engineering of Advanced Materials", FCI, and Office of Basic Energy Sciences of the US Department of Energy are gratefully acknowledged.

Supporting Information Available: Fluorescence spectra of **2** and **3**, data of nanosecond flash photolysis experiment for **3**, peak current−scan rate relationship for the bilayer of **4**, and photocurrent action spectra of **4** on ITO. These materials are available free of charge via the Internet at http://pubs.acs.org.

JA909970H